1993

Collaborating PDE Solvers with Interface Relaxation

Mo Mu

John R. Rice
Purdue University, jrr@cs.purdue.edu

Report Number:
93-024

COLLABORATING PDE SOLVERS WITH INTERFACE RELAXATION

Mo Mu
John R. Rice

CSD-TR-93-024
April 1993

COLLABORATING PDE SOLVERS WITH INTERFACE RELAXATION

MO MU* AND JOHN R. RICE†

Abstract. This paper deals with one of the well known domain decomposition methods, the collaborating PDE solvers approach. A class of relaxers based on interface relaxation are described. The convergence analysis is presented, and the optimal relaxation parameters are determined. This analysis applies directly to problems involving Laplace operators, Dirichlet boundary conditions, and domains that can be decomposed into rectangles so that each interior corner belongs to 4 rectangles (i.e., interior corners are cross points). The discretization used in the analysis is a five-point start finite differences on tensor product meshes. The extensions of the analysis to more general problems are discussed, the convergence can be established for more general operators (e.g., self-adjoint or varying from subdomain to subdomain), more general boundary conditions (e.g., mixed boundary conditions), more general geometry, and more general discretizations. We are not able to explicitly solve for optimum relaxation parameters for these extensions. Numerical results are also reported. We show that this is a very promising approach to solve complex PDEs on complex domains.

Key words. domain decomposition, interface relaxation, optimal relaxation parameters, iterative methods, partial differential equations, parallel computation

AMS(MOS) subject classifications. 65N55, 65F10, 65Y05

1. Introduction.

This paper deals with one of the well known domain decomposition methods, the collaborating PDE (*partial differential equation*) solvers approach. It applies to complex PDEs on complex domains. It consists of the following basic steps. (1) Decompose the entire domain into a collection of simply shaped subdomains. (2) Identify interface conditions at the boundaries of the simple subdomains that the overall PDE solution should satisfy. If the PDEs are solved on each simple subdomain and the interface conditions are satisfied, then the whole problem is solved. (3) Obtain PDE solvers that can solve the PDEs on the various simple subdomains. Different solvers can be used on different subdomains. (4) Devise relaxation formulas that move two neighboring PDE solutions toward satisfying the interface conditions. (5) Iterate solving the PDEs in the simple subdomains and relaxing the interface conditions until they are all satisfied.

While sharing many common merits with other domain decomposition methods, such as the use of existing efficient PDE solvers for step 3 and inherent massive parallelism, this approach has further attractions over other approaches. Most importantly, it is very loosely globally-glued. No single PDE is imposed on the entire domain; no PDEs are imposed on interfaces between subdomains; and no artificial overlapping is assumed among subdomains. We believe that this approach is a more reasonable simulation of the real world. In fact, the physical world has no "global" controller, it evolves by satisfying physical laws (PDEs) locally and by adjusting interfaces with neighbors. Another attraction is that it uses the object-oriented philosophy. The software modules for each simple domain can be encapsulated into an object that

* Computer Sciences Department, Purdue University, West Lafayette, IN 47907 U.S.A., mu@cs.purdue.edu, or na.mu@na-net.ornl.gov. Work supported in part by National Science Foundation grant CCR-8619817.

† Computer Sciences Department, Purdue University, West Lafayette, IN 47907 U.S.A., rice@cs.purdue.edu, or na.rice@na-net.ornl.gov. Work supported in part by the Air Force Office of Scientific Research grants, 88-0243, F49620-92-J-0069.

performs the tasks (e.g., displaying the domain, plotting its solution, solving its PDE, and relaxing its interface along a boundary). This approach thus allows one to reuse PDE solving software in an easy and natural way.

The challenge of this approach is to find relaxation formulas and iterations so the solution is obtained rapidly. Many ideas can be applied to construct relaxers. For example, as the extension of the classical Schwarz method – *alternate iteration with overlapping* [4], at each iteration the Dirichlet condition is imposed on one side of an interface and the Neumann condition on the other side. Its convergence is proved under some assumptions. Similarly, one can alternately impose the Dirichlet condition and the Neumann condition on the interface at every other iteration. A more general approach is to use a smoothing function to blend the solutions cross the interface by adjusting the physical interface conditions. However, the convergence mechanism is, in general, still not well understood for these relaxers. In order to explore this approach more fully, a RELAX system has been built [2] that is a software platform and user interface for creating complex problems and testing various relaxers. Experiments show that this collaborating PDE solvers approach is very promising and works for many relaxers and problems. Fig. 1.1 shows a physical heat flow problem that is successfully solved by the RELAX system. The complex object consists of seven simple subdomains with nine interfaces. The radiation conditions allow heat to leave on the left and bottom while the temperature U is zero on all the other boundaries. The mounting regions have heat dissipated. The interface conditions are continuity of temperature U and its derivative. Let U denote the temperature on "this" side of an interface and V the temperature on the "other" side. The relaxation formula used is then

$$U^{new} = \frac{U^{old} + V^{old}}{2} + \omega(U_n^{old} - V_n^{old}) \tag{1.1}$$

where ω is a relaxation parameter. Fig. 1.2 shows the solution computed after 15 iterations.

This paper presents a convergence analysis for this collaborating PDE solvers approach. Under certain model problem assumptions, the convergence can be proved for a class of relaxers and for general composite geometric domains consisting of rectangles. The optimal relaxation parameter is determined in some special cases.

The paper is organized as follows. Section 2 describes a general relaxation scheme. Section 3 presents the relaxation for a simple situation which is analyzed in Section 4. Section 5 describes how the analysis is extended to more general cases. Numerical results are reported on in Section 6. Finally, we give conclusions in Section 7.

2. Relaxation. Suppose that the complex domain Ω consists of k simply shaped subdomains $\Omega_1, \Omega_2, \ldots, \Omega_k$, with interfaces Γ_{ij} as the common boundary piece of Ω_i and Ω_j, i.e., $\Gamma_{ij} = \partial\Omega_i \cap \partial\Omega_j$. Each subdomain obeys a physical law locally, i.e., there is a PDE L_l and function U_l defined in each Ω_l so that

$$L_l U_l = f_l \quad \text{in } \Omega_l \quad \textit{for } l = 1, 2, \ldots, k. \tag{2.1}$$

The entire problem satisfies certain boundary conditions on $\partial\Omega$ with some given data. Inside Ω, the local solutions are glued together with certain interface conditions. More specifically, for each Γ_{ij} the interface condition can usually be specified by the form

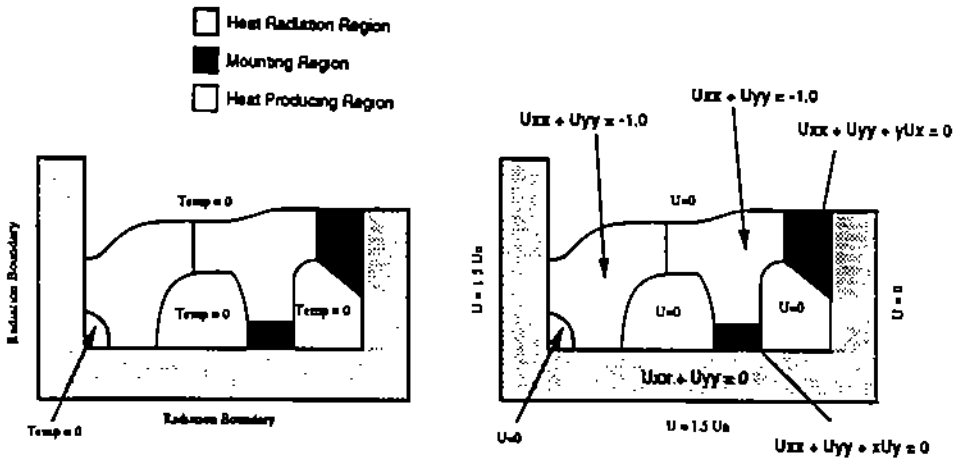

FIG. 1.1. *A physical heat flow problem for a complex domain along with the physical and mathematical descriptions.*

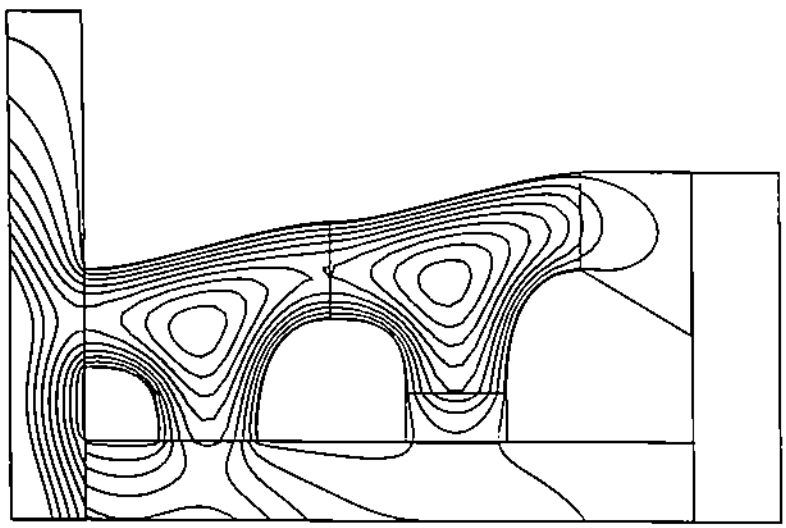

FIG. 1.2. *The contour plot of the solution computed after 15 iterations for the problem in Fig. 1.1.*

$$g_{ij}(U_i, U_j, \frac{\partial U_i}{\partial n}, \frac{\partial U_j}{\partial n}) \equiv 0 \tag{2.2}$$

For example, for the continuity conditions of the global solution and its normal derivative, (2.2) takes the form

$$(U_i - U_j)^2 + \left(\frac{\partial U_i}{\partial n} - \frac{\partial U_j}{\partial n}\right)^2 \equiv 0 \quad \text{on each } \Gamma_{ij}. \tag{2.3}$$

For some physical phenomena we might have different conditions to be satisfied on opposite sides of the interface so that the interface conditions need not be symmetric, i.e., we can have $g_{ij} \neq g_{ji}$. As mentioned in Section 1, there are many possible choices for the relaxation. We consider the following class of relaxers. First, we consider only *stationary relaxers*, those that use the same relaxation and PDE solution techniques at every iteration. There are non-stationary relaxers of serious interest, such as those that alternate between satisfying Neumann and Dirichlet conditions at the interfaces. Second, we consider only relaxers that use values and derivatives of PDE solutions along the interfaces. That is, at each iteration a PDE is solved for U_l in Ω_l and the boundary values of U_l and its derivatives are the input to the relaxers. Discrete versions of the relaxers may involve such values on or near the interfaces.

We define this class of relaxers precisely as follows. Let $I(l)$ be the indices of those subdomains that are neighbors of subdomain l. Let the PDE problem that is solved on Ω_l be

$$\begin{aligned} L_l U_l^{new} &= f_l && \text{in } \Omega_l, \\ B_{lj} U_l^{new} &= b_{lj} && \text{on } \Gamma_{lj} \text{ for } j \in I(l), \\ & U_l^{new} \text{ satisfies the global boundary conditions on } \partial\Omega, \end{aligned} \tag{2.4}$$

where B_{lj} is a usual boundary condition operator and b_{lj} is defined as part of the relaxer as follows. Let $\vec{X}_{lj}^{old}$ be a vector of values which approximate U_l and its derivatives on Γ_{lj} for $j \in I(l)$. The length of the vector $\vec{X}$ is the number of derivatives of U_l used, it is normally 2 (using values and normal derivatives of U_l). Then a *relaxer* is a procedure that maps U_l^{old}, $\vec{X}_{lj}^{old}$ for $j \in I(l)$, $\vec{X}_{jl}^{old}$ for $j \in I(l)$ into b_{lj}. Clearly the relaxer must incorporate some properties derived from (2.2) as its purpose is to better satisfy this condition. While relaxers are usually simple formulas like (1.1), they can also be complex procedures involving, for example, (a) solving special ordinary or partial differential equations along the interfaces, or (b) using various least square smoothing of functions along the interfaces.

When (2.4) is solved we obtain a set of solutions U_l^{new} for all subdomains for which, in general, $g_{ij}(U_i^{new}, U_j^{new}, \frac{\partial U_i^{new}}{\partial n}, \frac{\partial U_j^{new}}{\partial n})$ is not zero for each Γ_{ij}. We iterate by relaxing condition (2.2) with the relaxer and solving (2.4). We solve the entire problem by repeating this iteration until convergence.

In the remainder of this paper we consider rather simple relaxers and concentrate on studying convergence for somewhat general domains Ω and PDE operators L_l. We

believe that there are many and varied relaxers that are worthy of analysis and which might be effective in certain applications. Note that this definition of relaxers makes them domain-based and not interface-based. That is, the process of obtaining U_l^{new} is not easily interpreted as applying some independent set of procedures along the interfaces Γ_{lj} for $j \in I(l)$. Indeed, there might be interaction between different b_{lj} where, for example, two interfaces meet.

3. Matrix representation for a simple case. To be more specific and for the sake of simplicity, let us assume that Ω is as in Fig. 3.1 and denote $\Gamma_{i,i+1}$ simply by Γ_i. We present in Section 4 the convergence analysis for a special case where Ω is a rectangle and describe in Section 5 on how the analysis can be extended to an even more general composite domain with interior cross points as shown in Fig. 3.2.

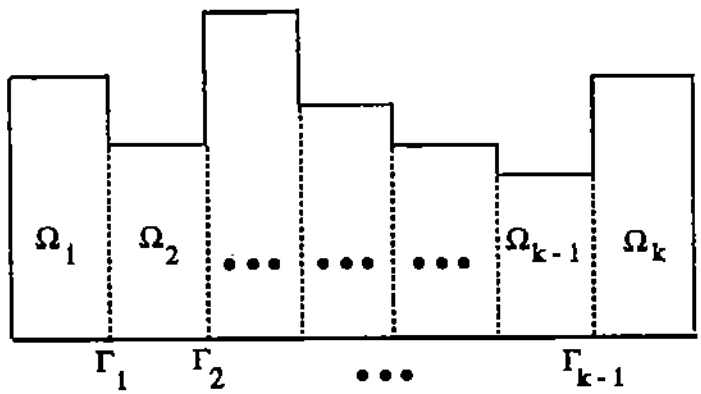

FIG. 3.1. *A "one dimensional" composite domain* Ω.

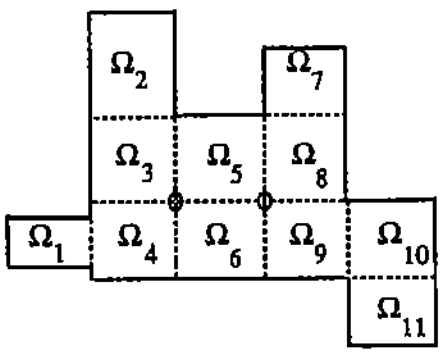

FIG. 3.2. *A general "two dimensional" composite domain with interior cross points (marked by "circles").*

Furthermore, without loss of generality, we assume that the global solution vanishes on $\partial\Omega$, and the interior interface condition is (2.3). Suppose we impose the Dirichlet condition on each Γ_{lj} for $j \in I(l)$ in (2.4). In our simplified notation, the solutions on both sides of any interface Γ_i have the same boundary values on Γ_i, denoted by X_i, at each iteration. Equation (2.3) is then reduced to

$$\frac{\partial U_i}{\partial n} \equiv \frac{\partial U_{i+1}}{\partial n} \quad \text{on } \Gamma_i \quad \textit{for } i = 1, 2, \ldots, k-1. \tag{3.1}$$

In principle, one can apply any numerical method, such as finite differences, finite elements, or collocation to solve the local PDE problem (2.4). The corresponding discrete systems can be generally written as

$$(3.2)\qquad \begin{cases} A_l U_l^{new} = f_l + P_{\Omega_l,\Gamma_{l-1}} X_{l-1}^{old} + P_{\Omega_l,\Gamma_l} X_l^{old} & for\ l = 1,2,\ldots,k \\ X_0^{old} \equiv X_k^{old} \equiv 0 \end{cases}$$

where the matrices A_l, $P_{\Omega_l,\Gamma_{l-1}}$ and P_{Ω_l,Γ_l} correspond to the discretization of the PDE operator L_l in the interior and next to the boundary pieces Γ_{l-1} and Γ_l of the subdomain Ω_l. Here and from now on, without confusion, we do not distinguish the notations for a continuous function and the vector of its discrete values.

After solving (3.2) to obtain $\{U_l^{new}\}_{l=1}^k$, we want to relax the interface conditions by adjusting the solution values on interfaces to better satisfy (3.1). Let $\{X_i^{new}\}_{i=1}^{k-1}$ denote the new interface values. The normal derivatives of the relaxed solutions on both sides of Γ_i can be approximated by the finite differences involving values on Γ_i and the discretization lines next to Γ_i. Denote these neighboring grid lines by $\Gamma_i^{\pm}$. A discrete approximation to (3.1) is then

$$(3.3)\qquad \frac{X_i^{new} - U_i^{new}|_{\Gamma_i^-}}{h_i^-} = \frac{U_{i+1}^{new}|_{\Gamma_i^+} - X_i^{new}}{h_i^+} \qquad for\ i = 1,2,\ldots,k-1,$$

where $h_i^{\pm}$ denote the corresponding spacings between Γ_i and $\Gamma_i^{\pm}$. Solving (3.3) for X_i^{new} we obtain

$$(3.4)\qquad X_i^{new} = \alpha_i^- U_i^{new}|_{\Gamma_i^-} + \alpha_i^+ U_{i+1}^{new}|_{\Gamma_i^+} \qquad for\ i = 1,2,\ldots,k-1,$$

with $\alpha_i^- = \frac{h_i^+}{h_i^- + h_i^+}$ and $\alpha_i^+ = \frac{h_i^-}{h_i^- + h_i^+}$. As in general relaxation methods, one can further introduce some relaxation parameters or make use of U_i^{new} and U_{i+1}^{new} values on other grid lines nearby Γ_i or use previous values X_i^{old}, U_i^{old}, etc., in order to accelerate the overall convergence. For example, one can define X_i^{new} by

$$(3.5)\qquad X_i^{new} = \omega X_i^{old} + (1-\omega)(\alpha_i^- U_i^{new}|_{\Gamma_i^-} + \alpha_i^+ U_{i+1}^{new}|_{\Gamma_i^+}),$$

where ω is a relaxation parameter. Recall that $X_i^{old} \equiv U_i^{new}|_{\Gamma_i} \equiv U_{i+1}^{new}|_{\Gamma_i}$ in the present case. In general, we see that a *linear relaxer* can be expressed as

$$(3.6)\qquad X_i^{new} = \varphi_i(U_i^{new}, U_{i+1}^{new}) \qquad \text{for } i = 1,2,\ldots,k-1,$$

where φ_i is a linear combination of U_i^{new} or U_{i+1}^{new} restricted to grid lines near to the interface Γ_i with certain weights. The choice of φ_i depends on the interface conditions (2.2), the approximation accuracy of the finite differences to the normal derivatives, the relaxation techniques, and so on.

We may combine solving (3.2) for $\{U_l^{new}\}_{l=1}^k$ with (3.6) to obtain the matrix representation of $\{X_i^{new}\}$ in terms of $\{X_i^{old}\}$. The convergence analysis of the relaxation

process is then reduced to the spectral analysis of the corresponding iteration matrix. More specifically, suppose the φ_i are defined by (3.5), and denote $P_{\Gamma_{i-1},\Omega_i}$ and P_{Γ_i,Ω_i} the matrices corresponding to the linear operators that restrict the solution in Ω_i to the grid lines next to Γ_{i-1} and Γ_i, respectively. Then, from (3.5) and (3.2) we have

$$
\begin{aligned}
X_i^{new} &= \omega X_i^{old} + (1-\omega)(\alpha_i^- P_{\Gamma_i,\Omega_i} U_i^{new} + \alpha_i^+ P_{\Gamma_i,\Omega_{i+1}} U_{i+1}^{new}) \\
&= \omega X_i^{old} + (1-\omega)\alpha_i^- P_{\Gamma_i,\Omega_i} A_i^{-1}(f_i + P_{\Omega_i,\Gamma_{i-1}} X_{i-1}^{old} + P_{\Omega_i,\Gamma_i} X_i^{old}) \\
&\quad +(1-\omega)\alpha_i^+ P_{\Gamma_i,\Omega_{i+1}} A_{i+1}^{-1}(f_{i+1} + P_{\Omega_{i+1},\Gamma_i} X_i^{old} + P_{\Omega_{i+1},\Gamma_{i+1}} X_{i+1}^{old}).
\end{aligned} \tag{3.7}
$$

Introduce the vector $\vec{X} = (X_1, X_2, \ldots, X_{k-1})$ of interface values, then (3.7) can be written in the matrix form

$$
\vec{X}^{new} = M\vec{X}^{old} + \vec{G} \tag{3.8}
$$

where $\vec{G}$ is a constant vector corresponding to $\{f_l\}$, $M = [B_i, D_i, C_i]$ is a $(k-1)\times(k-1)$ block tridiagonal matrix with

$$
\begin{aligned}
D_i &= \omega + (1-\omega)\alpha_i^- P_{\Gamma_i,\Omega_i} A_i^{-1} P_{\Omega_i,\Gamma_i} + (1-\omega)\alpha_i^+ P_{\Gamma_i,\Omega_{i+1}} A_{i+1}^{-1} P_{\Omega_{i+1},\Gamma_i} \\
&\quad for\ i = 1, 2, \ldots, k-1, \\
B_i &= (1-\omega)\alpha_i^- P_{\Gamma_i,\Omega_i} A_i^{-1} P_{\Omega_i,\Gamma_{i-1}} \quad for\ i = 2, \ldots, k-1, \\
C_i &= (1-\omega)\alpha_i^+ P_{\Gamma_i,\Omega_{i+1}} A_{i+1}^{-1} P_{\Omega_{i+1},\Gamma_{i+1}} \quad for\ i = 1, \ldots, k-2.
\end{aligned} \tag{3.9}
$$

Therefore, the convergence of the iteration with the interface relaxation is equivalent to

$$
\rho(M) < 1 \tag{3.10}
$$

where $\rho(\cdot)$ denotes the spectral radius.

4. Convergence analysis for a simple case. We now present the convergence analysis for the class of relaxers described in Section 3. In this section we consider the special case where Ω is a rectangle. In this case, the full spectrum of the matrix M can be obtained by the Fourier analysis so that the convergence mechanism is clearly understood. In addition, the optimal relaxation parameter analysis can also be performed directly. In the next section we prove the convergence for non-rectangular cases by a different argument.

We start with some model problem assumptions. Let the PDE operators L_l be Laplacian $(-\Delta)$ in all subdomains, let the global solution and its normal derivative be continuous on all interfaces. This is equivalent to solving the Poisson equation on the entire domain Ω with the same boundary condition on $\partial\Omega$. Furthermore, we assume that Ω is simply a rectangle and all subdomains in Fig. 3.1 have the same size. Each subdomain is discretized by a uniform tensor product grid with m vertical

and n horizontal interior grid lines and a spacing h. The PDE operator is discretized by the *5-point-star* finite differences, and the unknowns/equations are ordered using the natural indexing. The assumptions and analysis can be generalized to a separable and self-adjoint elliptic operator and a nonuniform grid. However, the analysis looks much more complicated even using essentially the same techniques, see [3].

Under the model problem assumptions, we have $A_l \equiv \frac{1}{h^2}A$, for $l = 1, 2, \ldots, k$, where $A = [-I, T, -I]$ is an $m \times m$ block tridiagonal matrix with $T = [-1, 4, -1]$ being an $n \times n$ tridiagonal matrix; $h^2 P^T_{\Omega_l,\Gamma_{l-1}} \equiv P_{\Gamma_{l-1},\Omega_l} \equiv V^T = [I, 0, \ldots, 0]^T$ and $h^2 P^T_{\Omega_l,\Gamma_l} \equiv P_{\Gamma_l,\Omega_l} \equiv W^T = [0, \ldots, 0, I]^T$ are $1 \times m$ block matrices with I denoting the $n \times n$ identity matrix; and, finally, $\alpha_i^- \equiv \alpha_i^+ = \frac{1}{2}$ for $i = 1, \ldots, k-1$. Then, relations (3.9) are reduced to

$$
\begin{array}{rcl}
D \equiv D_i & = & \omega + \frac{(1-\omega)}{2}(V^T A^{-1} V + W^T A^{-1} W) \quad \text{for } i = 1, 2, \ldots, k-1 \\
C \equiv C_i \equiv B_{i+1}^T & = & \frac{(1-\omega)}{2} V^T A^{-1} W \qquad\qquad\qquad\quad \text{for } i = 1, 2, \ldots, k-2.
\end{array}
\tag{4.1}
$$

LEMMA 4.1. *The matrices D and C can be expressed as functions of the matrix T as follows:*

$$
D = d(T), \quad C = c(T),
\tag{4.2}
$$

where the scalar functions $d(t)$ and $c(t)$ are defined as

$$
d(t) = \omega + \frac{(1-\omega)}{2}\left(t - \frac{c_m(t)}{s_{m-1}(t)}\right), \quad c(t) = \frac{(1-\omega)}{2 s_{m-1}(t)},
\tag{4.3}
$$

and $s_m(t)$ and $c_m(t)$ are Chebyshev polynomials defined by

$$
\begin{array}{rcl}
s_m(t) & = & \frac{\eta^{m+1} - \eta^{-(m+1)}}{\eta - \eta^{-1}} \qquad \eta = \frac{t}{2} + \sqrt{(\frac{t}{2})^2 - 1} \quad \text{for } t > 2. \\
c_m(t) & = & \eta^m + \eta^{-m}
\end{array}
\tag{4.4}
$$

Proof. Observe that the matrix $S \equiv T - V^T A^{-1} V - W^T A^{-1} W$ is the two-subdomain Schur complement on the interface. From [1] we have

$$
\begin{array}{rcl}
S & = & s_{m-1}^{-1}(T) c_m(T), \\
V^T A^{-1} W & = & s_{m-1}^{-1}(T).
\end{array}
\tag{4.5}
$$

Lemma 4.1 then immediately follows. □

LEMMA 4.2. *The eigenvalues of the matrix M can be expressed as*

$$\lambda_{ij} = \omega + \tfrac{(1-\omega)}{2} q_{ij} \quad \textit{for } i = 1,2,\ldots,k-1, \quad j = 1,2,\ldots,n \tag{4.6}$$

with

$$\begin{aligned} q_{ij} &= t_j - \tfrac{\eta_j^m + \eta_j^{-m} - 2\cos\frac{i\pi}{k}}{\eta_j^m - \eta_j^{-m}}(\eta_j - \eta_j^{-1}), \\ \eta_j &= \tfrac{t_j}{2} + \sqrt{(\tfrac{t_j}{2})^2 - 1}, \end{aligned} \tag{4.7}$$

where

$$t_j = 2 + 4\sin^2\frac{j\pi}{2(n+1)} \qquad \textit{for } j = 1,2,\ldots,n \tag{4.8}$$

are eigenvalues of the matrix T.

Proof. Let $p(\lambda)$ be the eigenpolynomial of M and $T = Q^T \Lambda Q$ be the eigendecomposition of T. Then from (4.2) we have

$$\begin{aligned} p(\lambda) &= \det(M - \lambda I) \\ &= \det[C^T, D - \lambda I, C] \\ &= \det[c(T), d(T) - \lambda I, c(T)] \\ &= (\det(Q))^{2(k-1)} \det[c(\Lambda), d(\Lambda) - \lambda I, c(\Lambda)] \\ &= (\det(Q))^{2(k-1)} \textstyle\prod_{j=1}^{n} \det[c(t_j), d(t_j) - \lambda, c(t_j)]. \end{aligned} \tag{4.9}$$

Thus, the eigenvalues of M are also the eigenvalues of the $(k-1)\times(k-1)$ tridiagonal matrices $[c(t_j), d(t_j), c(t_j)]$ for $j = 1,2,\ldots,n$, which, in turn, can be expressed as

$$\lambda_{ij} = d(t_j) - 2c(t_j)\cos\frac{i\pi}{k} \qquad \textit{for } i = 1,2,\ldots,k-1, \quad j = 1,2,\ldots,n. \tag{4.10}$$

This, combined with (4.3), establishes Lemma 4.2. □

LEMMA 4.3. *For any $1 \le i \le k-1$, $1 \le j \le n$ and $m > 1$, we have*

$$0 < q_{ij} < 2. \tag{4.11}$$

Proof. Observe that $t_j = \eta_j + \eta_j^{-1}$, so q_{ij} can be rewritten as

$$q_{ij} = \frac{2(\eta_j^{2m} - \eta_j^2 + \eta_j^2 \cos\frac{i\pi}{k} - \cos\frac{i\pi}{k})}{\eta_j(\eta_j^{2m} - 1)} \tag{4.12}$$

Because $t_j > 2$, we have $\eta_j > 1$ for $j = 1, 2, \ldots, n$. Therefore, to prove $q_{ij} > 0$, it suffices to show that

$$\eta^{2m} - \eta^2 + \eta^2 \cos y - \cos y > 0 \qquad \text{for } \eta > 1 \tag{4.13}$$

where $0 < y < \pi$. This follows by directly applying the standard calculus computation to verify that the left hand side, as a function of η, and its first three derivatives are increasing functions. Then a check of the boundary values at $\eta = 1$ establishes (4.13). Similarly, to prove $q_{ij} < 2$, one shows that

$$\eta^{2m} - \eta^2 + \eta^2 \cos y - \cos y < \eta(\eta^{2m} - 1) \tag{4.14}$$

or, equivalently,

$$\eta^{2m+1} - \eta^{2m} + \eta^2 - \eta^2 \cos y - \eta + \cos y > 0. \tag{4.15}$$

Inequality (4.15) then follows by the same argument as used for (4.13). This completes the proof of Lemma 4.3. □

We are now at the position to prove the theorem on the convergence of the relaxation and to determine the optimal iteration parameter for the class of relaxers. Let ω_{opt}^+, ω_{opt}^- be the optimal positive and negative iteration parameters, respectively, and let ρ_{opt}^+, ρ_{opt}^- be the corresponding values of $\rho(M)$.

THEOREM 4.4. *Let* $q_{\max} = \max_{ij} q_{ij}$, *and* $q_{\min} = \min_{ij} q_{ij}$. *Then we have*

$$(4.16)(1) \quad \rho(M) = \begin{cases} \omega + \frac{(1-\omega)}{2} q_{\min} & \text{for } \omega \geq 1, \\ \omega + \frac{(1-\omega)}{2} q_{\max} & \text{for } 0 \leq \omega \leq 1, \\ \max\left\{ |\omega + \frac{(1-\omega)}{2} q_{\max}|, |\omega + \frac{(1-\omega)}{2} q_{\min}| \right\} & \text{for } \omega \leq 0. \end{cases}$$

$$(2) \qquad \min_{\omega \geq 0} \rho(M) = \rho(M)|_{\omega=\omega_{opt}^+} = \frac{q_{\max}}{2} \left(\equiv \rho_{opt}^+ \right),$$

$$\omega_{opt}^+ = 0;$$

$$\begin{aligned} \min_{\omega<0} \rho(M) &= \rho(M)|_{\omega=\omega_{opt}^-} = \tfrac{q_{max}-q_{min}}{4-(q_{max}+q_{min})} \left(\equiv \rho_{opt}^-\right), \\ \omega_{opt}^- &= -\tfrac{q_{max}+q_{min}}{4-(q_{max}+q_{min})}. \end{aligned} \tag{4.17}$$

(3)
$$\rho_{opt}^- < \rho_{opt}^+ < 1;$$

$$\begin{aligned} \rho_{opt}^+ &= 1 + c_{\alpha,k} h + O\left(h^2\right); \\ \tfrac{\rho_{opt}^+}{\rho_{opt}^-} &\approx 1 + \tfrac{2-q_{max}}{2} = 1 + c_{\alpha,k} h + O\left(h^2\right), \end{aligned} \tag{4.18}$$

where the constant factor $c_{\alpha,k}$ depends on the number, k, of subdomains and the aspect ratio, $\alpha = \frac{m}{n}$, of each subdomain. The exact expression of $c_{\alpha,k}$ is given by (4.23) in the following proof of the theorem.

Proof. From Lemma 4.2 we have

$$\rho(M) = \max_{ij} |\omega + \frac{(1-\omega)}{2} q_{ij}|. \tag{4.19}$$

If $0 \leq \omega \leq 1$, recall that $q_{ij} > 0$, we get

$$\begin{aligned} \rho(M) &= \max_{ij}(\omega + \tfrac{(1-\omega)}{2} q_{ij}) \\ &= \omega + \tfrac{(1-\omega)}{2} \max_{ij} q_{ij} \\ &= \omega + \tfrac{(1-\omega)}{2} q_{max}. \end{aligned}$$

If $\omega \geq 1$, we can rewrite (4.19) as

$$\rho(M) = \max_{ij} |\frac{q_{ij}}{2} + \frac{\omega}{2}(2 - q_{ij})|.$$

Recall that $0 < q_{ij} < 2$ so we have

$$\begin{aligned} \rho(M) &= \max_{ij} \left(\tfrac{q_{ij}}{2} + \tfrac{\omega}{2}(2 - q_{ij})\right) \\ &= \max_{ij} \left(\omega + \tfrac{(1-\omega)}{2} q_{ij}\right) \\ &= \omega + \tfrac{(1-\omega)}{2} \min_{ij} q_{ij} \\ &= \omega + \tfrac{(1-\omega)}{2} q_{min}. \end{aligned}$$

If $\omega \leq 0$, we can view $\omega + \frac{(1-\omega)}{2} q_{ij}$ as points on a linear function of q: $y = \omega + \frac{(1-\omega)}{2} q$. So, the maximum is reached at one of the end points. That is,

$$\rho(M) = \max\{|\omega + \frac{(1-\omega)}{2}\max_{ij} q_{ij}|, \quad |\omega + \frac{(1-\omega)}{2}\min_{ij} q_{ij}|\}.$$

In fact, the formulas for $\omega \geq 0$ can also be viewed as two special cases of this general one. The proof of (4.16) is complete.

From (4.16), it is easy to see that

$$\begin{aligned} \min_{\omega \geq 1} \rho(M) &= \min_{\omega \geq 1} \left(\tfrac{q_{\min}}{2} + \tfrac{\omega}{2}(2 - q_{\min})\right) \\ &= \left(\tfrac{q_{\min}}{2} + \tfrac{\omega}{2}(2 - q_{\min})\right)|_{\omega=1} \\ &= 1; \end{aligned} \tag{4.20}$$

and

$$\begin{aligned} \min_{0 \leq \omega \leq 1} \rho(M) &= \min_{0 \leq \omega \leq 1} \left(\tfrac{q_{\max}}{2} + \tfrac{\omega}{2}(2 - q_{\max})\right) \\ &= \left(\tfrac{q_{\max}}{2} + \tfrac{\omega}{2}(2 - q_{\max})\right)|_{\omega=0} \\ &= \tfrac{q_{\max}}{2}, \end{aligned} \tag{4.21}$$

which gives the first part of (4.17). Assume $\omega \leq 0$, then to minimize $\max\{|\omega + \frac{(1-\omega)}{2}q_{\max}|; |\omega + \frac{(1-\omega)}{2}q_{\min}|\}$ we know that ω_{opt}^- has to satisfy the following equation:

$$|\omega_{opt}^- + \frac{(1-\omega_{opt}^-)}{2}q_{\max}| = |\omega_{opt}^- + \frac{(1-\omega_{opt}^-)}{2}q_{\min}|.$$

Solving this equation gives the second part of (4.17).

From (4.17) we have

$$\begin{aligned} \frac{\rho_{opt}^+}{\rho_{opt}^-} &= \frac{q_{\max}(4-(q_{\max}+q_{\min}))}{2(q_{\max}-q_{\min})} \\ &= \frac{4(q_{\max}-q_{\min})-q_{\max}^2-q_{\max}q_{\min}+4q_{\min}}{2(q_{\max}-q_{\min})} \\ &= 2 - \frac{q_{\max}^2+q_{\max}q_{\min}-4q_{\min}}{2(q_{\max}-q_{\min})}. \end{aligned} \tag{4.22}$$

Recall that $q_{\max} < 2$, so (4.22) then implies that

$$\frac{\rho_{opt}^+}{\rho_{opt}^-} > 2 - \frac{2q_{\max} + 2q_{\min} - 4q_{\min}}{2(q_{\max} - q_{\min})} = 1,$$

which, plus the fact that $\rho_{opt}^+ < 1$, proves the first relation of (4.18). Observe that $q_{\max}$ corresponds to $\eta_{\min}$, which, in turn, corresponds to $t_{\min}$. Since $t_{\min} = 2 + O(h^2)$,

we have $\eta_{\min} = 1 + \delta/n + O(h^2)$ and $\eta_{\min}^n = e^{n log \eta_{\min}} = e^{\delta}(1 + O(h))$, where δ is a constant. We rewrite the expression (4.12) for $q_{\max}$ as

$$q_{\max} = 2\left(1 + \frac{(\cos\frac{\pi}{k} - 1)(\eta_{\min}^2 - 1)}{\eta_{\min}^{2m} - 1}\right)/\eta_{\min}.$$

Using the Taylor's expansion for it, we get

$$q_{\max} = 2\left(1 + \frac{(\cos\frac{\pi}{k} - 1)(2\delta h + O(h^2))}{(e^{\delta\alpha} - 1)(1 + O(h))}\right)(1 - \delta h + O(h^2)),$$

which yields the second relation of (4.18) with

$$c_{\alpha,k} = \left(\frac{2(\cos\frac{\pi}{k} - 1)}{e^{\delta\alpha} - 1} - 1\right)\delta. \tag{4.23}$$

Finally, denoting $\epsilon = 2 - q_{\max}$ and using (4.22), we have

$$\begin{aligned} \frac{\rho_{opt}^+}{\rho_{opt}^-} &= 1 + \frac{\epsilon}{2} + \frac{\epsilon q_{\min}}{2-(\epsilon+q_{\min})} \\ &= 1 + \epsilon[\frac{1}{2} + \frac{q_{\min}}{2-(\epsilon+q_{\min})}]. \end{aligned} \tag{4.24}$$

Since $q_{\min} = O(h)$, it is easy to obtain the third relation of (4.18) from (4.24). The proof of Theorem 4.4 is thus complete. □

Theorem 4.4 states that the relaxation process diverges for all $\omega \geq 1$, and converges for $0 \leq \omega < 1$ with the optimal positive parameter at $\omega = 0$, which corresponds to the relaxation formula (1.1) with $\omega = 0$. In other words, any nonnegative parameter ω with the use of the old values on interfaces does not accelerate the convergence at all. However, using a negative parameter ω may accelerate the convergence if the optimal relaxation parameter is chosen properly. The relaxation formula (3.5) with $\omega < 0$ may be viewed as an approximation to the second order normal derivative condition on each interface, instead of the first order. In addition, the optimal convergence rates approach 1 linearly as the spacing h approaches 0, and the coefficient factors depend on the number k of subdomains from the term $\cos\frac{\pi}{k}$, and on the aspect ratio α of each subdomain from the term $(e^{\delta\alpha} - 1)^{-1}$. These results agree with the convergence behavior for most of the domain decomposition methods.

5. Convergence analysis for nonrectangular domains. This section extends the convergence analysis to nonrectangular domains as in Figures 3.1 and 3.2. For the sake of simple notation, we first consider the case of Fig. 3.1 and then show that the convergence theorem also holds for the case of Fig. 3.2.

We first notice that the linear operator relations (3.8) and (3.9) are true for the case of Fig. 3.1 with proper matrix representations for P_{Γ_i,Ω_j}, P_{Ω_j,Γ_i}, and A_i, as we display later on. To prove (3.10) for convergence, it suffices to show, using the Rayleigh principle, that

$$\vec{X}^T M \vec{X} < \vec{X}^T \vec{X} \quad \text{for all } \vec{X} \neq 0. \tag{5.1}$$

One key idea in our argument is to change the natural *interface-based* analysis as involved in (5.1) to the *subdomain-based* analysis, which then allows us to further extend the convergence analysis to general composite geometric domains no matter how interfaces are related to subdomains. For simplicity of notation, from now on we assume that no relaxation parameter is used, i.e., $\omega = 0$; and a uniform spacing h is also used so that $\alpha_i^+ \equiv \alpha_i^- \equiv \frac{1}{2}$.

LEMMA 5.1. *With the convention that $X_0 \equiv X_k \equiv 0$, for the expression of the left hand side of inequality (5.1) we have*

$$\vec{X}^T M \vec{X} = \frac{1}{2} \sum_{i=1}^{k} v_i, \tag{5.2}$$

with

$$v_i = [X_{i-1}^T, X_i^T] M_i \begin{bmatrix} X_{i-1} \\ X_i \end{bmatrix}, \tag{5.3}$$

where

$$M_i = \begin{bmatrix} P_{\Gamma_{i-1},\Omega_i} A_i^{-1} P_{\Omega_i,\Gamma_{i-1}} & P_{\Gamma_{i-1},\Omega_i} A_i^{-1} P_{\Omega_i,\Gamma_i} \\ P_{\Gamma_i,\Omega_i} A_i^{-1} P_{\Omega_i,\Gamma_{i-1}} & P_{\Gamma_i,\Omega_i} A_i^{-1} P_{\Omega_i,\Gamma_i} \end{bmatrix}. \tag{5.4}$$

Proof. The proof of Lemma 5.1 is done by simply using relation (3.9) and regrouping terms in the summation for the expression of $\vec{X}^T M \vec{X}$. This completes the proof. □

Let $m_i(n_i)$ be the number of interior vertical (horizontal) grid lines in Ω_i, and let l_j be the number of interior grid points on Γ_j. We have

$$l_j \leq n_i \quad \text{for } j = i-1 \text{ and } i, \tag{5.5}$$

because the interfaces Γ_{i-1} and Γ_i are parts of the vertical boundary pieces of Ω_i. Then for the 5-point star stencil, the four "P" operators in M_i have block matrix representations when ordered according to vertical grid lines and with "0" corresponding to a group of $m_i - 1$ lines,

$$\begin{aligned} h^2 P_{\Omega_i,\Gamma_{i-1}}^T \equiv P_{\Gamma_{i-1},\Omega_i} &= [H_{i,i-1}^T, 0]^T, \\ h^2 P_{\Omega_i,\Gamma_i}^T \equiv P_{\Gamma_i,\Omega_i} &= [0, H_{i,i}^T]^T; \end{aligned} \tag{5.6}$$

where the $n_i \times l_j$ matrix $H_{i,j}$ has the form

$$H_{i,j} = \begin{bmatrix} 0 \\ I_j \end{bmatrix} \qquad \text{for } j = i-1,\ i \tag{5.7}$$

with I_j being the $l_j \times l_j$ identity matrix.

LEMMA 5.2. *For each subdomain Ω_i, we have*

$$\rho(M_i) < 1, \qquad i = 1, 2, \ldots, k. \tag{5.8}$$

Proof. Let $\{A_i^{-1}\}_{\alpha,\beta}$ denote the block at the position (α, β) in the corresponding block partion of A_i^{-1}, we have

$$\begin{aligned} M_i &= \begin{bmatrix} H_{i,i-1}^T & 0 \\ 0 & H_{i,i}^T \end{bmatrix} \begin{bmatrix} \{A_i^{-1}\}_{1,1} & \{A_i^{-1}\}_{1,m_i} \\ \{A_i^{-1}\}_{m_i,1} & \{A_i^{-1}\}_{m_i,m_i} \end{bmatrix} \begin{bmatrix} H_{i,i-1} & 0 \\ 0 & H_{i,i} \end{bmatrix} \\ &\equiv \tilde{H}_i^T \tilde{M}_i \tilde{H}_i. \end{aligned} \tag{5.9}$$

From Theorem 2.1 in [1], we can express $\tilde{M}_i$ as

$$\tilde{M}_i = \begin{bmatrix} f_i(T_i) & g_i(T_i) \\ g_i(T_i) & f_i(T_i) \end{bmatrix}, \tag{5.10}$$

where $T_i = [-1, 4, -1]_{n_i \times n_i}$, $f_i(t) = s_{m_i-1}(t)/s_{m_i}(t)$ and $g_i(t) = 1/s_{m_i}(t)$. Therefore, the eigenvalues of $\tilde{M}_i$ are given by

$$\begin{aligned} \tilde{\lambda}_{ij} &= f_i(t_j) \pm g_i(t_j) \\ &= \tfrac{s_{m_i-1}(t_j) \pm 1}{s_{m_i}(t_j)}, \qquad t_j \in \sigma(T_i). \end{aligned}$$

Similar to the argument in the proof of Lemma 4.3, one can easily verify that

$$0 < \tilde{\lambda}_{ij} < 1. \tag{5.11}$$

With the notations used in (5.7) and (5.9), we observe that M_i is simply the matrix expanded from a principal submatrix of $\tilde{M}_i$. So, we have

$$0 \le \sigma(M_i) < 1. \tag{5.12}$$

This is another key idea that enables the extension of the convergence analysis to cases where an interface can be a portion of a vertical or horizontal boundary piece for a subdomain. The proof of the lemma is thus complete. □

THEOREM 5.3. *The relaxation process converges in the case of Fig. 3.1. An upper bound on the convergence rate is*

$$\rho = \max_{1 \le j \le k-1} \left[\frac{\rho(M_j) + \rho(M_{j+1})}{2} \right]. \tag{5.13}$$

Proof. From (5.3) and (5.12) we have

$$0 \le v_i \le \rho(M_i)(X_{i-1}^T X_{i-1} + X_i^T X_i). \tag{5.14}$$

Substituting (5.14) into (5.2) for each v_i and regrouping the terms in the summation in terms of interfaces, we obtain

$$\begin{aligned} 0 \;&\le\; \vec{X}^T M \vec{X} \le \textstyle\sum_{j=1}^{k-1} \left(\frac{\rho(M_j)+\rho(M_{j+1})}{2} \right) X_j^T X_j \\ &\le\; \rho \vec{X}^T X. \end{aligned} \tag{5.15}$$

Using inequality (5.8), we have

$$\rho < 1. \tag{5.16}$$

This completes the proof. □

We can extend Theorem 5.3 to the important more general case of Fig. 3.2 by taking a closer look at the previous argument. If a subdomain Ω_i has both vertical and horizontal interfaces as boundary pieces, we can obtain a partition of M_i similar to (5.4) if we introduce for each direction x or y a matrix M_i^x or M_i^y. Correspondingly, the binary form v_i in (5.3) becomes a sum of two parts, one for each direction. Similarly, we use for each interface Γ_{ij} the notation

$$\rho_{ij} = \begin{cases} \frac{\rho(M_i^x)+\rho(M_j^x)}{2} & \text{if } \Gamma_{ij} \text{ is a vertical interface} \\ \frac{\rho(M_i^y)+\rho(M_j^y)}{2} & \text{if } \Gamma_{ij} \text{ is a horizontal interface.} \end{cases} \tag{5.17}$$

THEOREM 5.4. *The relaxation process also converges in the case of Fig. 3.2. The convergence rate is bounded above by*

$$\rho \;=\; \max_{\Gamma_{ij}} \rho_{ij} \;<\; 1. \tag{5.18}$$

Proof. We notice that Fig. 3.2 extends Fig. 3.1 in three ways. First, both vertical and horizontal interfaces may be present. Lemma 5.1 and Lemma 5.2 are then

naturally extensible by using the previous observation with (5.17) and the eigenvalue analysis for M_i^x and M_i^y, respectively. Second, there may be an interface, say $\Gamma_{1,4}$, that is a middle portion of a boundary piece of a subdomain. In this case, the H-matrix defined in (5.7) may take the form $[0, I_j, 0]^T$. However, it is easy to see that this does not affect the argument in Lemma 5.2 to obtain (5.12). Finally, for the interior "cross points" as marked by "circles" in Fig. 3.2, we note that they are, in fact, not involved in the computation because the 5-point-start stencil does not use these boundary corner points for the subdomains around them. This completes the proof of Theorem 5.4. □

For the record, we formally state the result that can be established using the same line of argument as above.

COROLLARY 5.5. *Theorems 5.3 and 5.4 remain true for non-uniform mesh spacing and for* $w \neq 0$.

We further comment on other possible extensions of the convergence analysis. First, we note that the quantity v_i can be viewed as a discrete approximation of a boundary integral for the subdomain Ω_i:

$$v_i = \int_{\partial\Omega_i} \int_{\partial\Omega_i} U_i(\xi)\rho_i(\xi,\eta)U_i(\eta)d\xi\, d\eta, \tag{5.19}$$

where the interface value function $U_i(s) \equiv 0$ on $\partial\Omega \cap \partial\Omega_i$, i.e., the support of $U_i(s)$ is only on the interior interfaces; $\rho_i(x,y)$ corresponds to a Poisson kernel. There are many ways one may obtain an analog to relation (5.14), namely

$$0 \leq v_i \leq \rho(\Omega_i)||U_i||^2_{\partial\Omega_i}, \qquad \text{with } \rho(\Omega_i) < 1, \tag{5.20}$$

using elliptic PDE theory. These usually involve a *maximum-value principle* for more general PDE operators, geometric domains, non-tensor-product meshes, and discretization methods. Then, the remaining argument for the convergence analysis just follows trivially. Second, one may also extend the relaxation parameter analysis to general cases although it is usually not feasible to obtain simple, explicit formulas for the optimum parameters. Since the properties of individual subdomain problems may vary, one, however, has to apply different parameters to different interfaces. The optimal parameter choice problem then becomes a multivariate linear programming analysis.

6. Numerical experiments. In this section, we report on some experiments to illustrate the convergence behavior of the relaxation process. The experiments are performed under the model problem assumptions in Section 4.

Table 1 shows selected values for the optimal parameter ω_{opt}^- and its corresponding convergence rate ρ_{opt}^-; and the convergence rate ρ_{opt}^+ corresponding to $\omega_{opt}^+ = 0$. Seven cases are examined with various numbers, n, m and k, of the interior horizontal or vertical grid lines, and the subdomains, respectively. They reflect the changes in spacing, aspect ratio and decomposition. The corresponding values for $q_{\min}$ and $q_{\max}$ as defined in Theorem 4.4 are also listed that determine ω_{opt}^-, ρ_{opt}^- and ρ_{opt}^+.

TABLE 1

Selected values for the optimal parameter ω_{opt}^- and the corresponding convergence rate ρ_{opt}^-; and the convergence rate ρ_{opt}^+ corresponding to $\omega_{opt}^+ = 0$. Here n is the number of interior horizontal grid lines in each subdomain; m is for the interior vertical grid lines; and k is the number of subdomains. $q_{\min}$ and $q_{\max}$ are the quantities defined in Theorem 4.4 that determine ω_{opt}^-, ρ_{opt}^- and ρ_{opt}^+.

Case	n	m	k	$q_{\min}$	$q_{\max}$	ω_{opt}^-	ρ_{opt}^-	ρ_{opt}^+
1	30	30	11	0.3438	1.825	− 1.18	0.809	0.913
2	50	50	11	0.3434	1.891	− 1.27	0.877	0.946
3	150	150	11	0.3432	1.962	− 1.36	0.955	0.981
4	30	30	21	0.3438	1.826	− 1.19	0.810	0.913
5	30	30	501	0.3438	1.826	− 1.19	0.810	0.913
6	50	30	11	0.3434	1.913	− 1.29	0.900	0.957
7	50	10	11	0.3434	1.959	− 1.36	0.952	0.980
8	50	2	11	0.0135	1.956	− 0.97	0.957	0.978

TABLE 2

Maximum error ($e_{\max}$) after 25 iterations for solving a Poisson equation. The initial error is 9.924. Various relaxation parameter values for ω are tested, including the optimum one, $\omega_{opt}^- = -1.136$.

ω	− 1.200	− 1.136	− 1.000	0.500	0.000
$e_{\max}$	6.237e-3	4.567e-3	1.275e-2	2.896	0.678

We observe that the convergence with ω_{opt}^- is always faster than that with $\omega_{opt}^+ \equiv 0$. By checking cases 1 through 3, we see how the convergence is slowed down as the spacing h decreases. Comparison of cases 1, 4 and 5 shows that the convergence is very insensitive to the number of subdomains, which is extremely important for massively parallel computation. Finally, by checking cases 2, 6, 7 and 8, we see that the convergence is also affected by the aspect ratio, m/n, of subdomains. Thus, very thin or fat subdomains are not recommended.

To investigate the convergence sensitivity to the choice of relaxation parameter, we solve a Poisson equation with Dirichlet condition on the rectangular domain $\Omega = (1,4) \times (0,1)$. The true solution is chosen as $U(x,y) = x^2 + y^2$ so that no discretization error is present. The domain Ω is decomposed into three subdomains with interfaces at $x = 2$ and $x = 3$. A uniform grid, with $n = m = 27$, is used for each subdomain. The theoretical values for ω_{opt}^-, ρ_{opt}^- and ρ_{opt}^+ are -1.136, 0.766 and 0.89, respectively. Various relaxation parameter values for ω are examined to see the effect on convergence. Table 2 lists the corresponding values for the maximum error, $e_{\max}$, on Ω after 25 iterations. The initial error is 9.924. We observe that the convergence rate is not very sensitive to the accuracy of ω_{opt}^-.

For comparison, we solve the same problem on a bigger domain $\Omega = (1,12) \times (0,1)$ with 11 unit square subdomains. In this case, $\omega_{opt}^- = -1.139$, $\rho_{opt}^- = 0.775$ and $\rho_{opt}^+ = 0.89$. The initial error is 121.9. With ω_{opt}^- and ω_{opt}^+, the errors are reduced after 25 iterations to 0.290 and 8.487, respectively. We see that the convergence rates remain about the same as the last example as the number of subdomains changes from 3 to 11.

7. Conclusions. We have presented the convergence analysis for a class of relaxers based on the interface relaxation in collaborating PDE solvers. Optimal relaxation parameters are determined theoretically under certain model problem assumptions. Extensions to more general and complex cases are discussed and convergence of the relaxation is proved. Both theoretical and experimental results show that the collaborating PDE solvers approach is very promising to solve complex PDEs on complex domains. It also allows one to easily implement this approach using modern software technologies, especially on massively parallel computing environments.

REFERENCES

[1] R.E. Bank and D.J. Rose (1977), *Marching algorithms for elliptic boundary value problems. I: the constant coefficient case*, SIAM J. Numer. Anal., 14, pp. 792–829.

[2] McFadden, H.S., and John R. Rice (1992), *Collaborating PDE solvers*, Appl. Numer. Math., 10, pp. 279–295.

[3] M. Mu and J.R. Rice (1992), *Preconditioning for domain decomposition through function approximation*, CSD-TR-92-091 and CER-92-42, Department of Computer Sciences, Purdue University, West Lafayette, IN47907, December, Submitted to SIAM J. Sci. Comput..

[4] A. Quarteroni and G. Sacchi-Landriani (1988), *Domain decomposition preconditioners for the spectral collocation method*, NASA Contractor Report 181620, ICASE Report No. 88-11, ICASE, NASA Langley Research Center, Hampton, VA 23665.